Wu et al. Int J Concr Struct Mater (2019) 13:8
https://doi.org/10.1186/s40069-018-0307-y

International Journal of Concrete Structures and Materials

RESEARCH Open Access

Experimental Study on Waterproofing Properties of Putty-Based Composite Rubber Strip for Underground Post-Tensioned Precast Concrete Structures

Xiang-guo Wu[1,2], Xiao-kai Chen[1], Shi-yan Yu[1], Seongwon Hong[3*] and Thomas H.-K. Kang[4]

Abstract

The proper assembly of underground precast concrete structures is often critical in the construction of underground structures. In particular, interfacial waterproofing between precast concrete segments is a key factor influencing use, safety, and life span. Current practice is to incorporate waterproofing rubber strips in the design. During the installation process, compressive stress is applied to the strip by post-tensioning to achieve performance. For this paper, lateral constraint compression tests were carried out on composite rubber seal strips that utilize putty. Special waterproofing and sealing test devices were designed to investigate corresponding relationships between water pressure and compressive stress (or strain). A relationship between water resistance pressure and compression stress and strain of the putty-based composite rubber strip was proposed based on the series tests and the control target of the minimum compression strain of the putty composite rubber strip was then suggested. Finally, full-scale waterproofing tests on tunnel joints were conducted. The experimental results provide a scientific reference for the engineering application and design of composite sealing rubber strips putty for underground post-tensioned precast concrete structures.

Keywords: full-scale tests, joints, precast concrete structure, putty-based composite rubber strip, waterproofing, post-tensioning

1 Introduction

Waterproofing is typically a key design goal for underground precast concrete structures (Ossai 2017). For modern tunnel structures, segments often require casting of high performance concrete with very low permeability (DAUB 2013). Therefore, the primary possible leakage point considered is the segmental joint (Yurkevich 1995; Lee and Ge 2001; Henn 2010; Wang et al. 2011; Wu et al. 2014; Fang et al. 2015; Soltani et al. 2018). For tunnel lining, one of the most significant factors impacting the overall behavior and structure response was the existence of the segmental joints for precast concrete units (Wood 1975; Koyama 2003). Due to the underground environment, repair after the leakage in the structure is very difficult. In general, design service life for underground structures ranges from 75 to 100 years. Structures within urban underground tunnel networks tend to deform due to the long-term dynamic load and impacts associated with surrounding buildings. Under working conditions, the largest deformation was frequently observed and entered into failure state at the joint (Böer et al. 2014; Huang et al. 2015; Hong et al. 2016). Therefore, waterproofing materials need to accommodate structural deformation.

In present concrete construction, elastic rubber strips in sealing and waterproofing joints of assembling segments have been commonly used. For underground concrete structures, standard design for sealing joints

*Correspondence: shong@ut.ac.kr
[3] Department of Safety Engineering, Korea National University of Transportation, Chungju, Chungbuk, South Korea
Full list of author information is available at the end of the article
Journal information: ISSN 1976-0485 / eISSN 2234-1315

uses Ethylene-Propylene-Diene Monomer (EPDM) polymer rubber strips arranged circumferentially on the end faces of the segment (Ding et al. 2017). Putty-based composite rubber strips have great viscosity and elasticity, which can compensate to a certain degree for the adverse effect of the interface defects at joints. To evaluate the waterproofing ability at joints, special attention is directed to the sealant behavior of the EPDM sealing strips. A time-dependent constitutive model is proposed to assess the long-term waterproof ability of EPDM rubber used in segmental joints (Shi et al. 2015). At present, there are few requirements for rubber strips in the design specifications, and there is limited understanding of the relationship between applied forces and waterproofing performance. In addition, precast concrete structures incorporate a groove at the joint interface for the rubber strip positioning (Hu et al. 2009). The type of groove at the joint interface can limit rubber strip lateral deformation, which can increase pressure on the strip and improve waterproofing ability. The various types of grooves offer different degrees of constraint. Therefore, mechanical properties of rubber strips along with groove design at precast concrete structure joints are key elements in waterproof design. The joint open width is also regarded as a key performance indicator, since it is the weakest part of the shield segmental lining (Liao et al. 2008; Zhang et al. 2015). As the weakest and vulnerable point in the segmental lining, joints have been investigated in experiments (Ding et al. 2013; Liu et al. 2015; Kiani et al. 2016), numerical analyses (Ding et al. 2004; Teachavorasinskun and Chub-uppakarn 2010) and case studies (Jun 2011; Basnet and Panthi 2018). Testing apparatus was designed to accurately monitor water leakage pressure of segmental joints under various combinations of opening and offsets (Ding et al. 2017). Molins and Arnau (2011) presented an in situ load test and 3D numerical simulation on a full-scale segmental lining for the Barcelona metro line. According to a case study in Shanghai, Huang et al. (2017) perceived that longitudinal joints of the metro tunnel have large open widths and lose waterproofing when disrupted by unexpected surcharges.

In this paper, mechanical tests for compressive stress and strain of putty-based composite rubber strips along with waterproofing performance tests at the interface between putty-based composite rubber strips and concrete are conducted. These tests investigate influence of strip compressive force and the joint stretching value on waterproofing of sealing rubber strips. It attempts to establish a design model and proposed control target for mechanical and waterproofing properties of this new type of rubber strip. Waterproofing test of a full-scale tunnel joint is carried out. The research work of this paper provides a scientific reference for the engineering application and design of composite sealing rubber strips with putty for underground post-tensioned precast concrete structures.

2 Experimental Methods

2.1 Compression Tests of Putty-Based Composite Rubber Strip Under Constraint

The putty-based composite rubber strip was made up of Ethylene-Propylene-Diene Monomer polymer rubber (EPDM foam strip) and the external composite layer (putty paste) of high viscosity reactive polymer cement (butyl rubber). The primary reason for use of the composite was to take advantage of the external putty-based material's properties of viscosity and superplasticity, which can heal mesoscopic cracks and defects on the surface of concrete structures to improve interface waterproof ability. Cross section dimensions and picture of the rubber strip are shown in Fig. 1.

Figure 2 displays the lateral confinement loading test device, which is composed of two parts: convex shape of the upper part and concave shape of the lower part. The inner and outer diameter of the annular groove was 170 mm and 220 mm, respectively. The upper part has protrusion that squeezes the strip, and the annular groove is set at the lower part of the device with an annular rubber strip installed in it (see Fig. 2c). The length of the EPDM foam rubber in the elastic state has 640 mm, and the compression area is 15,315 mm^2. Quasi-stress control was selected for the tests.

2.2 Compression Tests to Design the Joint Interface of Precast Concrete Segment

It was assumed that the sealing effect of the rubber strip was based on the unique elasticity and resilience of the rubber. So that sealing was dependent on the resilience of the rubber seal. As the rubber strip was loaded, large elastic deformation was required. The elastic deformation

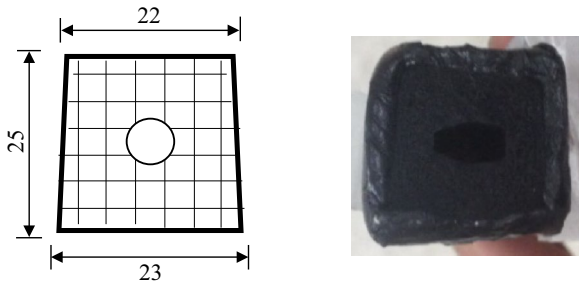

a Dimension of cross section **b** Rubber strip

Fig. 1 Putty based composite rubber strip: **a** dimension of cross section; and **b** rubber strip (units are in mm).

Fig. 2 Device of lateral confinement loading.

of the rubber helped keep its sealing property. According to Fan et al. (2002), the design parameter of the interface groove demonstrated in Eq. (1) is the area ratio,

$$\omega = \frac{A_s}{A_g} \tag{1}$$

where A_s is the cross-sectional area of the strip and $A_g$is the cross-sectional area of the interface groove. To investigate the influence of the precast concrete interface groove on the compression performance of the putty-based composite strip, two typical groove depths of 4 mm and 6 mm were used as shown in Fig. 3. The dimension of the two grooves was $40 \times 34 \times 4$ mm (occupying 26.3% of the strip with ω of 3.80) and $40 \times 34 \times 6$ mm (occupying 39.5% of the strip with ω of 2.53), respectively. The size of the precast concrete specimen was $100 \times 100 \times 300$ mm.

2.3 Laboratory Waterproofing Tests Using Putty-Based Composite Rubber Strip

In the post-tensioned precast concrete structure joint, waterproofing of the rubber sealing strip is achieved by assembling force and elastic restoring force. In short, compression performance of the sealant and bonding performance at the concrete interface are key factors that influence waterproofing performance. Figure 4 displays the schematic diagram and layout of the laboratory experimental device for waterproofing performance. The groove size was $40 \times 34 \times 6$ mm. Experimental devices

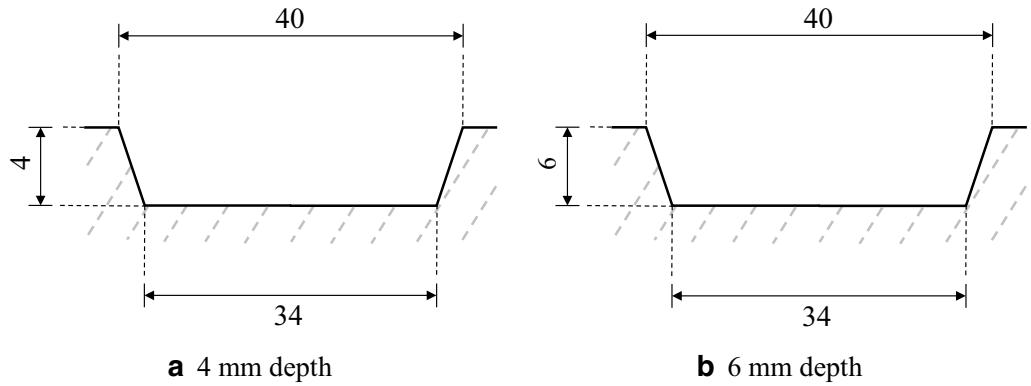

a 4 mm depth **b** 6 mm depth

Fig. 3 Two different sizes of precast concrete interface groove: **a** 4 mm depth; and **b** 6 mm depth (units are in mm).

mainly consisted of a universal testing machine with a capacity of 100 tons, upper and lower concrete compression plates, four dial gauges in the 50 mm range, Vernier calliper, 150 mm diameter pump pressure gauge (range of 1 MPa with division value of 5×10^{-3} MPa), three-way pipes, and control pump. The tests consisted of six loading levels based on different water pressures. Water was injected after each loading stage. Once reaching the water pressure, changes of hydraulic water pressure and compressive stress were measured.

2.4 Full-Scale Waterproofing Tests of Tunnel Joints

Full-scale waterproofing tests were carried out to evaluate whether the sealing strip at the junction of tunnels can achieve the designed water pressure. Figure 5 presents the schematic diagram of geometry (4100×9000 mm) and location of the post-tensioning steel bars. Two sections of the box culvert were constructed with the longitudinal length of 1500 mm. The full-scale waterproofing specimen is exhibited in Fig. 6. The dimension and shape of the putty-based composite rubber strip used in the full-scale test was $23 \times 22 \times 25$ mm with a hole in the middle of the cross section as shown in Fig. 1. Two strips were arranged in the joints with a combined total length of about 50 m. The groove surface was required to be clean before setting the sealing strip. In the two grooves of the culvert, the rubber strip was arranged in advance and the strip position was fixed by brushing chloroprene rubber glue in the grooves. Six post-tensioning steel bars were used to connect the two tunnel sections together and compress the sealing strip to make the joints waterproof. Once the strip was installed, the two box segments were assembled by post-tensioning the steel bars to bring them in contact with the strip in the groove clamped between. Subsequently, formal post-tensioning was started.

3 Results and Discussion

3.1 Compression Tests of Putty-Based Composite Rubber Strip Under Constraint

Experimental results of the putty-based composite strip under lateral confinement for compressive stress and displacement are provided in Fig. 7. At the early stage of loading, the compressive stress of the composite strip gradually increased with the displacement. It was observed that the displacement dramatically increased and at the later stage of the loading when the load reached at 112.36 kN primarily maintained at 11 mm. At end of the test, the rubber strip was not crushed and the internal EPDM foam rubber after unloading almost recovered to its original shape. The maximum displacement of the putty-based composite rubber strip under lateral confinement was approximately 11 mm, which was brought on by the squeezing of the inner hole of the composite strip raising the internal pore of the EPDM rubber. The instantaneous elastic recovery during the unloading process was 85% of total deformation. The residual deformation of the composite rubber strip was gradually recovered to its original state with time. Eventually, the rubber strip was not damaged. The deformation recovery of the inner elastic material to its original shape can partly drive unrecoverable external putty material.

3.2 Compression Tests to Design the Joint Interface of Precast Concrete Segment

In the loading process, the two end faces of the rubber strip were partially extruded upon loading, since they were not restrained at the end face (see Fig. 8). When maximum deformation was reached, the upper and lower parts of the concrete were in contact with each other.

Since deformation of the rubber strip was large and the contact area of the strip changed under incomplete constraint, the compressive force per unit length of the rubber strip was defined as compressive stress. The mean

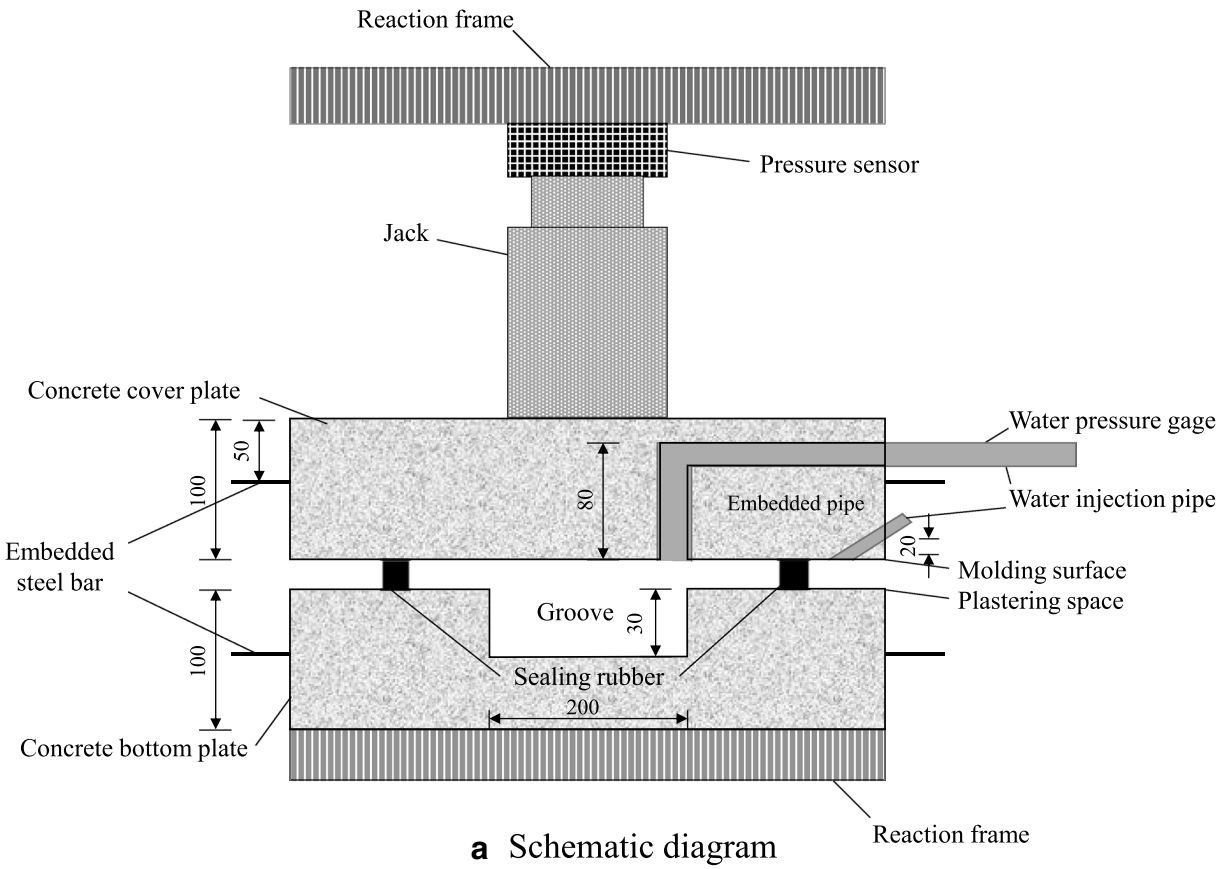

Fig. 4 Waterproofing experimental device: **a** schematic diagram; and **b** layout (units are in mm).

values of the experimental results of compressive stress and compression strain of the rubber strip are shown in Fig. 9.

There was an inflection point in the curves of the rubber strip in the two different grooves, as presented in Fig. 10. Before the point, the internal pore and middle hole of the sealing strip were not tightly compressed signifying that the compression strain increased gradually with compressive stress. Moreover, the relationship between compressive stress and compression strain for

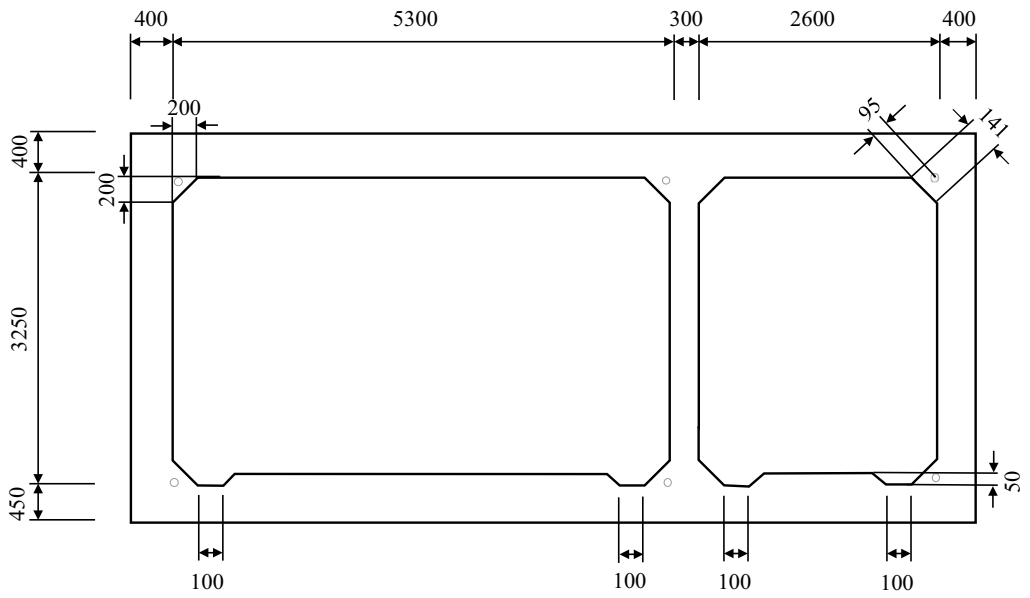

a Geometry

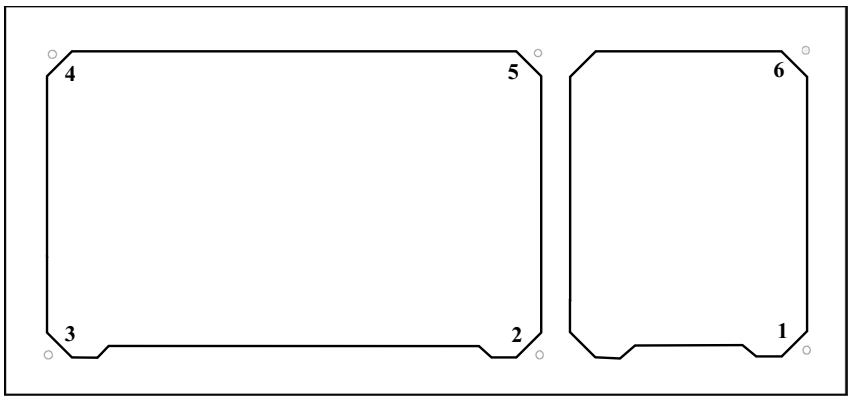

b Location of six tensioning steel bars

Fig. 5 Schematic diagram of full-scale waterproofing test: **a** geometry; **b** location of post-tensioning steel bars (units are in mm).

the two different sizes of groove were almost the same before the inflection point. At the inflection point, the central hole of sealing strip and the pore of foam rubber were completely compressed. The whole strip was so dense that the compressive force increased sharply with the compression strain. The compressive stresses of the sealing strip in the two different grooves at the inflection points were almost the same and their corresponding compression strain differed by roughly 20%.

In the early stage of compression, the compression moduli of the rubber strip were almost the same under the two groove constraints. In the later stage of loading, the compression stress of 6 mm depth of groove was greater than that of 4 mm depth under the same compression strain, and the compressive strain of the 4 mm depth of groove was greater than that of the 6 mm depth of groove under the same stress. This was mainly attributed to the difference in the constraint degree of the groove to the strip at the later stage of loading. In the final stage, the two compression interfaces of the 6 mm depth specimens were close in contact with each other. The remaining space at the joint was rather small, and there was no compression space. However, there was still a large space between the two interfaces of the 4 mm deep specimens. This was mainly due to the sum of the strip deformation and groove depth limit. The bilinear outsourced line was taken as an

Overview of the specimen before assembly

Installation of post-tensioning steel bars and the equipment after assembly

Sealing part of the specimen

Assembly process after installation of the putty-based composite rubber strip

Fig. 6 Full-scale waterproofing tests using the putty-based composite rubber strip.

approximate stress-deformation relation model as shown in Eq. (2),

$$\sigma_r = \frac{P}{L} = \begin{cases} E_0(\delta - \delta_i) & \delta_i \le \delta \le \delta_0 \\ E_0(\delta_0 - \delta_i) + E_h(\delta - \delta_0) & \delta > \delta_0 \end{cases} \tag{2}$$

where E_0 is the initial modulus, E_h is the hardening modulus, and δ_i is the initial compression strain, δ_0 is the characteristic compression strain. The experimental results of the model characteristic parameters are shown in Table 1.

The influence coefficient of the groove constraint is defined,

$$\psi = \frac{\delta_{0,4}}{\delta_{0,6}} \tag{3}$$

where $\delta_{0,4}$ is compression strain for 4 mm depth of the groove at unloading in E_h, and $\delta_{0,6}$ is the compression strain for 6 mm depth of the groove at unloading in E_h presented in Fig. 11. This coefficient can be used to characterize the relative influence of the groove depth on the constraint degree of the putty-based compound rubber strip.

3.3 Laboratory Waterproofing Tests

Figure 12 displays the experimental results of the laboratory waterproofing performance of the putty-based composite sealing rubber strip. The relationship between extrusion stress and water pressure was shown in Fig. 12a, and the strain and hydraulic water pressure behavior was drawn in Fig. 12b. The relationship between the compressive stress and the compression strain of rubber strip with the design value of water pressure was displayed in Eqs. (4) and (5).

$$\sigma_r = \frac{P}{L} = 8.92e^{(3p_w)} - 8.62\ (\text{kN/m}) \tag{4}$$

$$\delta = 68\left[1 - e^{(-9.67p_w)}\right]\ (\%) \tag{5}$$

where P_w is the water pressure (MPa). The minimum interface stress in the specification for waterproof elastic gasket of precast concrete tunnel joint was not applicable for the putty-based composite rubber strip. From the results of the waterproofing test, the minimum compression strain of the composite rubber strip for engineering purpose was 60% and the corresponding compressive stress was 10 kN/m.

3.4 Full-Scale Waterproofing Tests

The tests started with two culverts gradually assembled in place. After initial post-tensioning, dial gauges were installed inside the culverts to measure joint space variations in the process of post-tensioning. Simultaneously, the strains on the post-tensioning steel bars were recorded. The water injection pump and water pressure gauges at the lower part of the water injection hole of the box culvert were installed. After the steel bars were set in the duct, the conductor was run through the perforated sheet. The sheet was tightly attached to the concrete surface and bolts fastened. Table 2 provides experimental results of the post-tensioning process. The upper and lower prestressed steel bars were tensioned at the same time, otherwise the friction resulted in the vertical location due to the friction at the bottom so that the two tendons were employed. Upon completion of a post-tensioning cycle, the gap change and steel strain were measured. The bolts were then fastened.

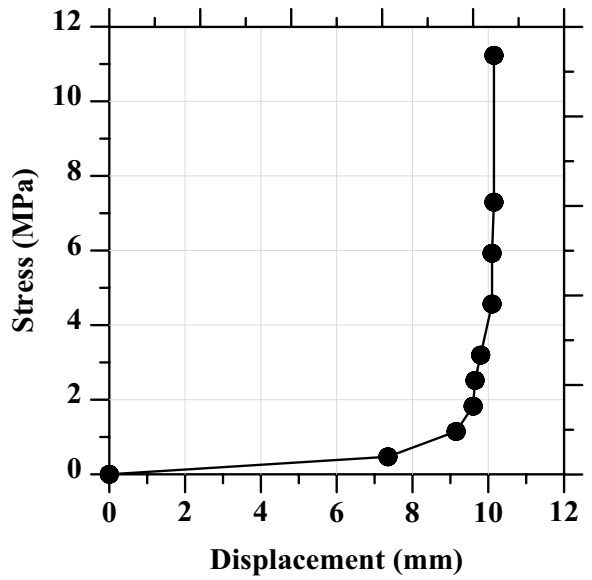

Fig. 7 Stress-displacement diagram for the putty based composite rubber strip in the compression test.

The maximum tension force was 180 kN. During the post-tensioning process, strain of steel bars varied linearly, indicating that the post-tensioned steel bars were in the elastic state with strain close to the theoretical value.

The width of the joints between the two box culverts was measured after the presetting tensioning steps. The results of the four fixed measurement points are shown in Table 3. The reason for the use of 3, 6, and 9 steps out of total 9 steps, which correspond to the last step of each post-tensioning cycle, was due to the determination time of the same width.

Because of errors at the interface of the whole joint, there were gaps between the maximum joint width and the minimum joints width in different places along the joint. Epoxy resin and chloroprene rubber glue were brushed in the groove, making the groove depth less than 6 mm. According to preliminary measurements, the depth of the groove was reduced by 2 mm, and the compression strain calculated by the average value was approximately 52%. At the same time, stress of the post-tensioning steel bars was monitored using strain gauges. The maximum stress loss of the steel bars before and after fastening the bolts was taken. As the post-tensioning steel bars were tensioned and the bolts fastened to a maximum value of 40 MPa and the minimum value of 10 MPa, the difference of displacement among the steel bars was 50–200 μm. Water injection by pressure pump was completed after tensioning to the presetting loading levels. Every pressure level was maintained up to 10–15 min.

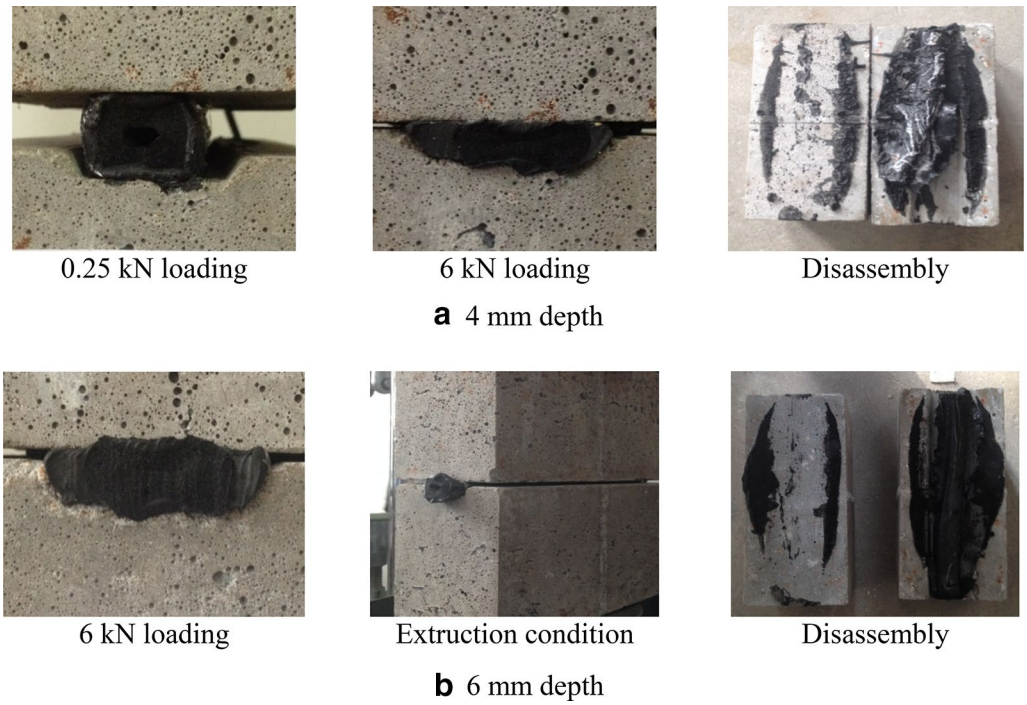

Fig. 8 Waterproofing tests: **a** 4 mm depth; and **b** 6 mm depth.

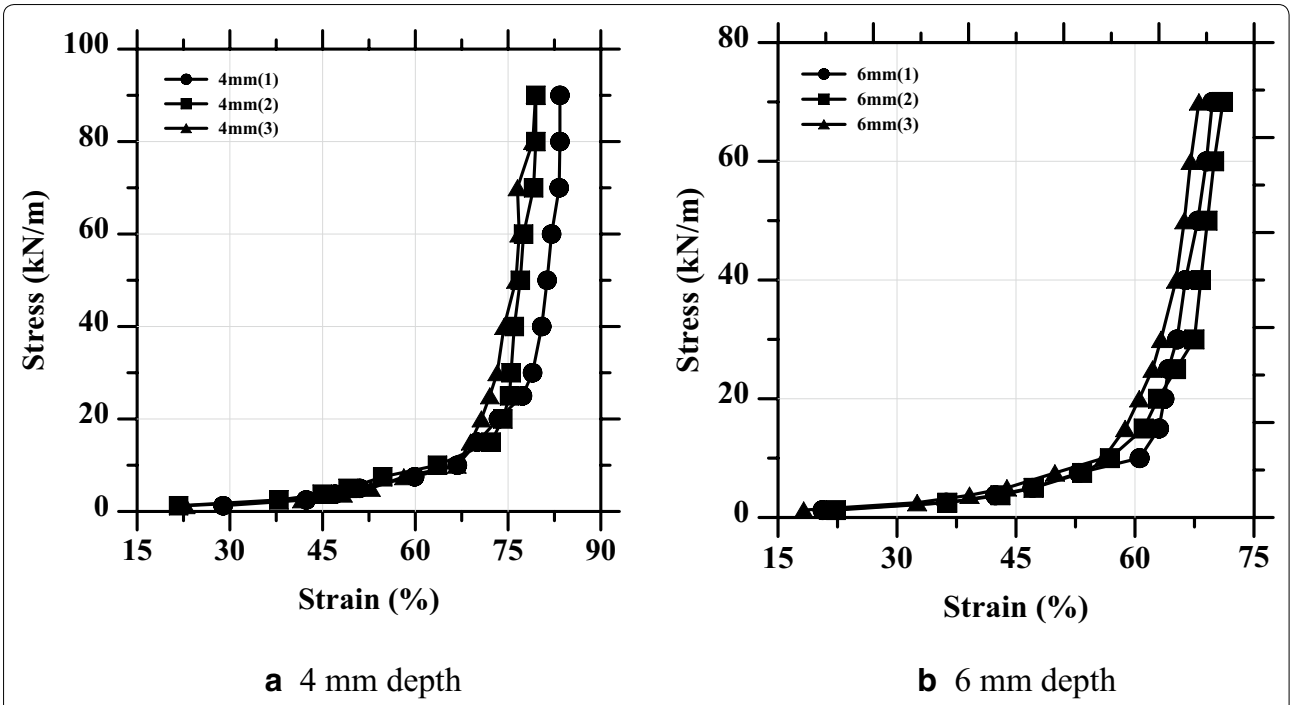

Fig. 9 Test results of the compression test for the putty-based composite rubber strip: **a** 4 mm depth; and **b** 6 mm depth.

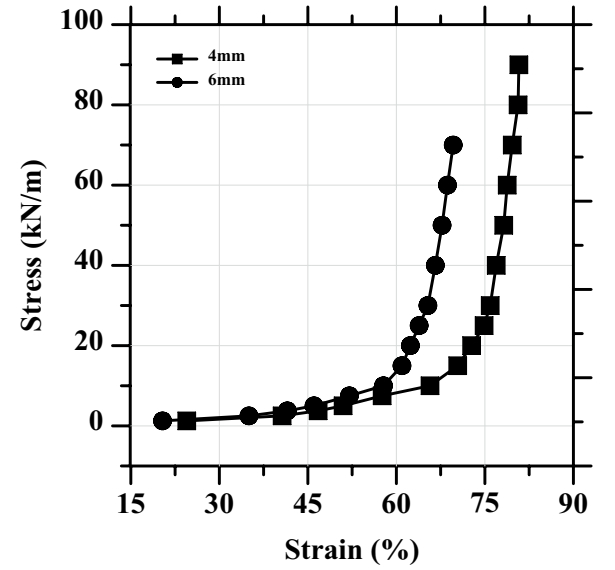

Fig. 10 Mean value of the compression test for two different sizes of the groove.

Table 1 Parameters of the bilinear stress-deformation relation model.

	4 mm	6 mm
E_0 (N/mm^2)	1.01	1.12
E_h (N/mm^2)	45.17	38.00
δ_i (%)	24.48	20.36
$(P/L)_i$ (kN/m)	1.25	1.25
δ_u (%)	80.6	69.6
$(P/L)_u$(kN/m)	80	70
δ_0 (mm)	74.76	63.6
$(P/L)_0$ (kN/m)	13.95	13.36

To observe whether there was leaking at the joint surface (Ministry of Housing and Urban Rural Development of People's Republic of China 2012). During this period, the water pressure value was allowed to decrease due to permeable water absorption on the concrete surface. Waterproofing was judged to fail once water droplets exuded from the joints and the surrounding concrete surface upon repressing when water pressure was reduced. The design value of water resistance pressure of this test was 0.12 MPa. During the test, the water pressure in the interface was gradually increased to 0.06, 0.08, 0.1 MPa and the design value of 0.12 MPa. Results indicated that there were no leakages at the interface of the strip denoting waterproofing ability of the sealing rubber strip in the joint interface was qualified under the designed water resistance pressure of 0.12 MPa.

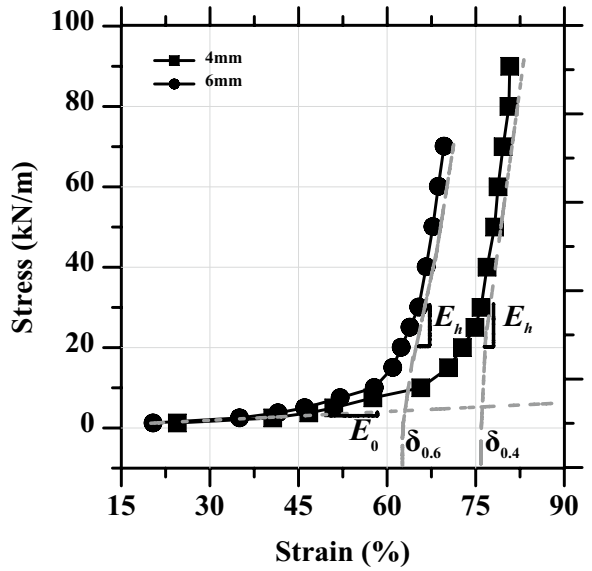

Fig. 11 Bilinear model for the experimental results of the compression tests.

4 Conclusions

In order to investigate the waterproofing performance of the putty-based composite rubber, mechanical behavior tests using rubber strip and waterproofing performance tests of the interface between the strip and precast concrete were performed. In addition, waterproofing test of a full-scale post-tensioned tunnel joint was carried out with the following conclusions drawn:

1. The compression performance of two different groove thicknesses (depths of 4 mm and 6 mm with ω of 3.80 and 2.53, respectively) with putty-based composite rubber strip was investigated in the tests under complete lateral restraint, and the compression characteristics of the putty-based composite rubber strip were obtained. The interface design parameters of groove constraints were employed to characterize the influence of groove size on the constraints to rubber strip in the compression process. The design parameters of the interface had an effect on the physical relationship between the compression stress of the strip and the compression strain.
2. According to the experimental analysis, the relationships between water resistance pressure and compression stress (or strain) of the putty-based composite rubber strip were proposed as shown in Eq. (4). The compression displacement or compression strain of the rubber strip by post-tensioning can be calculated from the relationship model and the design value of the water resistance pressure as displaced in Eqs. (4) and (5).

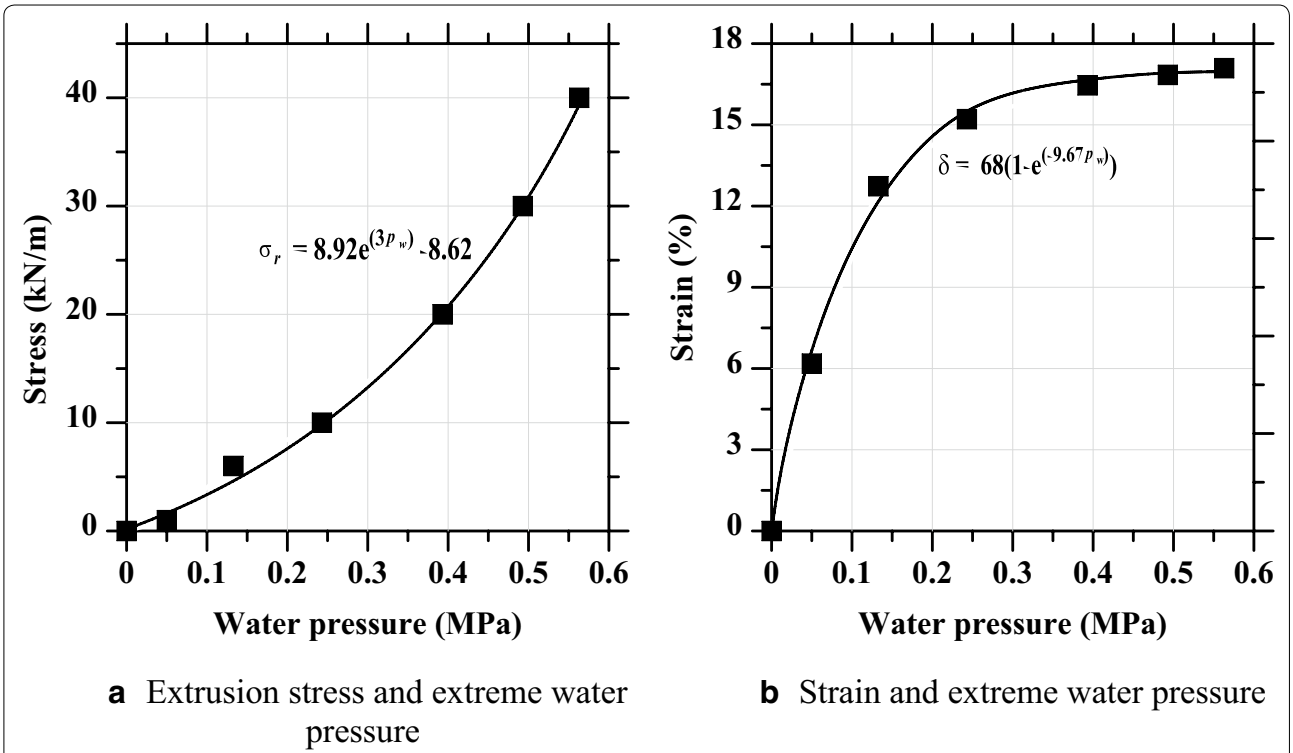

a Extrusion stress and extreme water pressure

b Strain and extreme water pressure

Fig. 12 Water resistance relationship between: **a** extrusion stress and extreme water pressure; **b** strain and extreme water pressure.

Table 2 Post-tensioning process of steel bars.

Post-tensioning steps	ID of post-tensioning bar	Stress at 1st pressure gauge (MPa)	Stress at 2nd pressure gauge (MPa)	Post-tensioning tensile force (kN)
1	1,6	20.7	20.1	100
2	3,4	20.7	20.1	100
3	2,5	20.7	20.1	100
4	1,6	29	28.2	140
5	3,4	29	28.2	140
6	2,5	29	28.2	140
7	1,6	37.27	36.26	180
8	3,4	37.27	36.26	180
9	2,5	37.27	36.26	180

Table 3 Experimental data of width of the joint.

Post-tensioning step	Width of the joints (mm)				Mean value (mm)
	Joint1	Joint 2	Joint 3	Joint 4	
Initial value	20.26	19.06	23.58	24.51	21.85
3	14.63	14.11	11.74	13.98	13.62
6	12.73	12.36	9.14	9.68	10.98
9	10.10	8.28	7.13	6.76	8.06

3. Based on the ratio of the compression deformation to the initial height of the rubber strip, the compression strain can be calculated. According to waterproofing tests, it was suggested as the control target that the minimum compression strain of the putty composite rubber strip for engineering purpose was 60% and the corresponding compressive stress was 10 kN/m. Compared with the traditional control target of interface stress, this target was more useful.

Authors' contributions
This work is not applicable for these sections. All authors read and approved the final manuscript.

Author details
[1] Key Lab of Structures Dynamic Behavior and Control of the Ministry of Education and School of Civil Engineering, Harbin Institute of Technology, Harbin, China. [2] Key Lab of Smart Prevention and Mitigation of Civil Engineering Disasters of the Ministry of Industry and Information Technology, Harbin Institute of Technology, Harbin, China. [3] Department of Safety Engineering, Korea National University of Transportation, Chungju, Chungbuk, South Korea. [4] Department of Architecture and Architectural Engineering, Seoul National University, Seoul, South Korea.

Acknowledgements
The authors would like to thank the following funds, fund providers or project team for supporting the authors' experimental work described herein: National Natural Science Foundation of China (51878222 and 51678196); Fundamental Research Funds for the Central Universities (Grant No. HIT. NSRIF. 2013112); Research and Development Project of the Ministry of Housing and Urban–Rural Development of P.R.C (K92017039); National Research Foundation of Korea (2017R1C1B5017487 and 2018R1A4A1025953); and NSFC-NRF joint collaborative fund (China Grant No. 51811540401 and Korea Grant No. 2018K2A9A2A06011014).

Competing interests
The authors declare that they have no competing interests.

Availability of data and materials
This work is not applicable for these sections.

Contest for publication
This work is not applicable for these sections.

Ethics approval and consent to participate
This work is not applicable for these sections.

Funding
This work is not applicable for these sections.

Publisher's Note

Received: 24 May 2018 Accepted: 27 September 2018
Published online: 28 January 2019

References
Basnet, C. B., & Panthi, K. K. (2018). Roughness evaluation in shotcrete-lined water tunnels with invert concrete based on cases from Nepal. *Journal of Rock Mechanics and Geotechnical Engineering, 10*(1), 42–59.

Böer, P., Holliday, L., & Kang, T. H.-K. (2014). Interaction of environmental factors on fiber-reinforced polymer composites and their inspection & maintenance: A review. *Construction and Building Materials, 50,* 209–218.

DAUB. (2013). *Recommendations for the design, production and installation of segmental rings* (p. 52). Germany: German Tunnelling Committee (ITA-AITES), Cologne.

Ding, W., Gong, C., Mosalam, K., & Soga, K. (2017). Development and application of the integrated sealant test apparatus for sealing gaskets in tunnel segmental joints. *Tunnelling and Underground Space Technology, 63,* 54–68.

Ding, W. Q., Peng, Y. C., Yan, Z. G., Shen, B. W., Zhu, H. H., & Wei, X. X. (2013). Full-scale testing and modeling of the mechanical behavior of shield TBM tunnel joints. *Structural Engineering and Mechanics, 45*(3), 337–354.

Ding, W.Q., Yue, Z.Q., Tham, L.G., Zhu, H.H., Lee, C.F., Hashimoto, T. (2004). Analysis of shield tunnel. *International Journal for Numerical & Analytical Methods in Geomechanics, 28* (1), 57–91.

Fan, Q. G., et al. (2002) . Experimental Study on the Waterproof Capability of the Hydro-expansive Rubber Sealing Cushion in Shield Tunnel. *Underground Space, 22*(4), 335–338. (in Chinese).

Fang, Q., Zhang, D., Li, Q. Q., & Wong, L. N. Y. (2015). Effects of twin tunnels construction beneath existing shield-driven twin tunnels. *Tunnelling and Underground Space Technology, 45,* 128–137.

Hong, W. P., Hong, S., & Kang, T. H.-K. (2016). Lateral earth pressure on a pipe buried in soft grounds undergoing lateral movement. *Journal of Structural Integrity and Maintenance*, *1*(3), 124–130.
Henn, R. W. (2010). *Practical guide to grouting of underground structures* (p. 191). Reston: ASCE.
Hu, X., Xue, W. C., & Wang, H. D. (2009). Waterproof test of PPMT joints in the 2010 Shanghai Expo area. *Special Structures, 26*(1), 109–113 (in Chinese).
Huang, H. W., Gong, W. P., Khoshnevisan, S., Juang, C. H., Zhang, D. M., & Wang, L. (2015). Simplified procedure for finite element analysis of the longitudinal performance of shield tunnels considering spatial soil variability in longitudinal direction. *Computers and Geotechnics, 64,* 132–145.
Huang, H. W., Shao, Hua, Zhang, D. M., & Wang, F. (2017). Deformational responses of operated shield tunnel to extreme surcharge: A case study. *Structure and Infrastructure Engineering, 13*(3), 345–360.
Jun, S. (2011). Durability problems of lining structures for Xiamen Xiang'an subsea tunnel in China. *Journal of Rock Mechanics and Geotechnical Engineering, 3*(4), 289–301.
Kiani, M., Akhlaghi, T., & Ghalandarzadeh, A. (2016). Experimental modeling of segmental shallow tunnels inalluvial affected by normal faults. *Tunnelling and Underground Space Technology*, *51*, 108–119.
Koyama, Y. (2003). Present status and technology of shield tunneling method in Japan. *Tunnelling and Underground Space Technology, 18*(2–3), 145–159.
Lee, K. M., & Ge, X. W. (2001). The equivalence of a jointed shield-driven tunnel lining to a continuous ring structure. *Canadian Geotechnical Journal, 38*(3), 461–483.
Liao, S. M., Peng, F. L., & Shen, S. L. (2008). Analysis of shearing effect on tunnel induced by load transfer along longitudinal direction. *Tunnelling and Underground Space Technology, 23,* 421–430.
Liu, X., Bai, Y., Yuan, Y., Mang, H.A. (2015). Experimental investigation of the ultimate bearing capacity ofcontinuously jointed segmental tunnel linings. Structure and Infrastructure Engineering, 1–16.
Ministry of Housing and Urban Rural Development of People's Republic of China. (2012). *National standard of People's Republic of China: Standard of test method of concrete structures*. Beijing: China building industry press.
Molins, C., & Arnau, O. (2011). Experimental and analytical study of the structural response of segmental tunnel linings based on an in situ loading test. Part 1: Test configuration and execution. *Tunnelling and Underground Space Technology, 26,* 764–777.
Ossai, C. I. (2017). Fitness-for-purpose evaluation of corroded pipelines using finite element analysis and fractural reliability estimation. *Journal of Structural Integrity and Maintenance, 2*(4), 209–216.
Soltani, M., Shakeri, E., & Zarrati, A. R. (2018). Development of a risk management model for power tunnels design process. *Journal of Structural Integrity and Maintenance*, *3*(1), 67–74.
Shi, C., Cao, C., Lei, M., Peng, L., & Shen, J. (2015). Time-dependent performance and constitutive model of EPDM rubber gasket used for tunnel segment joints. *Tunnelling and Underground Space Technology, 50,* 490–498.
Teachavorasinskun, S., & Chub-uppakarn, T. (2010). Influence of segmental joints on tunnel lining. *Tunnelling and Underground Space Technology, 25*(4), 490–494.
Wang, R., Xiao, T., & Yan, Z. (2011). Water leakage treatment and deformation control of shield tunnel in Shanghai metro. *Underground Engineering and Tunnels, S2,* 102–108 (in Chinese).
Wood, A. M. (1975). The circular tunnel in elastic ground. *Geotechnique, 25*(1), 115–127.
Wu, H.-N., Huang, R.-Q., Sun, W.-J., Shen, S.-L., Xu, Y.-S., Liu, Y.-B., et al. (2014). Leaking behavior of shield tunnels under the Huangpu River of Shanghai with induced hazards. *Natural Hazards, 70*(2), 1115–1132.
Yurkevich, P. (1995). Developments in segmental concrete linings for subway tunnels in Belarus. *Tunnelling and Underground Space Technology, 10*(3), 353–365.
Zhang, D. M., Huang, H. W., Hu, Q. F., & Jiang, F. (2015). Influence of multi-layered soil formation on shield tunnel lining behavior. *Tunnelling and Underground Space Technology, 47,* 123–135.